Liver Metastases: 3D Shape–based Analysis of CT Scans for Detection of Local Recurrence after Radiofrequency Ablation[1]

Ivan Bricault, MD, PhD
Ron Kikinis, MD
Paul R. Morrison, MS
Eric vanSonnenberg, MD
Kemal Tuncali, MD
Stuart G. Silverman, MD

This HIPAA-compliant pilot study had internal review board approval; informed consent was waived. The purpose was to determine retrospectively the diagnostic performance of a computer-aided three-dimensional (3D) analytic tool for assessing local recurrences of liver metastases by quantifying shape changes in ablated tumors on computed tomographic (CT) scans for follow-up of radiofrequency (RF) ablation. Positron emission tomographic and long-term CT follow-up images were reference standards. Fifty-six follow-up CT scans of 12 liver metastases (mean size, 4.0 cm) in nine patients treated with RF ablation were retrospectively analyzed. After the 1st month following RF ablation, the 3D analytic tool helped quantify ablated tumor shape variations and revealed recurrences even in the absence of abnormal enhancement (sensitivity, seven of seven; specificity, three of five). The 3D tool would have revealed a recurrence before it was reported clinically in two patients. Although results are preliminary, a 3D analytic tool based on shape may be useful in assessing RF ablation results.

Supplemental material: *http://radiology.rsnajnls.org/cgi/content/full/2411050987/DC1*

[1] From the Department of Radiology, University Hospital Michallon, BP 217, 38043 Grenoble, France (I.B.); TIMC-IMAG-CNRS Laboratory, Grenoble, France (I.B.); and Department of Radiology, Brigham and Women's Hospital, Boston, Mass (R.K., P.R.M., E.v.S., K.T., S.G.S.). Received June 13, 2005; revision requested August 3; revision received November 1; accepted November 23; final version accepted December 22. Supported in part by a study grant from the French Radiological Society. **Address correspondence to** I.B. (e-mail: *Ivan.Bricault@imag.fr*).

Percutaneous image-guided radiofrequency (RF) ablation is a minimally invasive alternative to surgical resection for the treatment of liver tumors (1–3). RF ablation involves delivery of high-frequency alternating current through a needle electrode to induce local coagulation necrosis (4). Although the value of magnetic resonance (MR) imaging has been investigated (5), contrast material–enhanced computed tomography (CT) is typically used to follow up patients and to determine if the treatment was successful in completely ablating the tumor. In general, successfully ablated tumors appear as nonenhancing areas (6). Unsuccessfully ablated tumors, or tumors that have recurred locally, typically manifest as areas of nodular or rim enhancement at contrast-enhanced CT (6). However, some recurrent liver tumors, particularly nonhypervascular metastases, demonstrate little, if any, abnormal enhancement (7). Chopra et al (8) showed that 37% of recurrent metastases manifested only as a change in tumor shape, with no discernible difference in enhancement between fully ablated and recurrent tumors. Detection of subtle changes in tumor shape can be challenging with two-dimensional CT scans alone. Thus, the purpose of our study was to retrospectively determine the diagnostic performance of a computer-aided three-dimensional (3D) analytic tool for assessment of local recurrences by quantifying shape changes in ablated tumors on follow-up CT scans, with positron emission tomographic (PET) and long-term CT follow-up images as the reference standard.

Advances in Knowledge

- A computer-aided three-dimensional (3D) analytic tool proved helpful in analyzing the shape of ablated liver tumors at several follow-up time points after percutaneous radiofrequency (RF) ablation.
- Although the 3D analysis demonstrated similar shape variations in recurrent and nonrecurrent tumors during the 1st month after RF ablation, it enabled recurrences to be detected after the 1st month even in the absence of abnormal enhancement.

Materials and Methods

Subjects and Imaging Data

Medical records and image data of patients who underwent percutaneous CT-guided RF ablation at Brigham and Women's Hospital between November 2000 and March 2003 were reviewed retrospectively under a medical records protocol approved by our internal review board. The study was compliant with the Health Insurance Portability and Accountability Act, and informed consent was waived. We used the Cool-tip RF Ablation System with Cluster Electrodes (Radionics, Burlington, Mass). We identified nine patients with 12 liver metastases (mean diameter, 4.0 cm) who satisfied the following criteria: *(a)* They had undergone CT-guided RF ablation of any number of liver metastases during a single session, performed with the intention to ablate the tumors completely; *(b)* they had undergone at least three successive follow-up contrast-enhanced CT examinations after ablation; and *(c)* complete ablation of metastases known to be revealed by PET with a high degree of sensitivity was confirmed with negative PET results (Table).

Portal phase images from 56 follow-up contrast-enhanced CT scans (performed a mean of 6.8 months after ablation [range, 0–24 months]) were reviewed. CT scans were obtained with a four–detector row CT scanner (Volume Zoom; Siemens Medical Solutions, Forchheim, Germany) or a 16–detector row CT scanner (Sensation 16; Siemens Medical Solutions). Detector collimation was 2.5 and 1.5 mm for the four– and 16–detector row scanners, respectively. For all scans, tube potential was 120 kV, tube current–time product was 160 mAs, pitch was 1.00–1.25, section thickness was 5 mm, and reconstruction increment was 5 mm.

Three-dimensional Analysis

A computer-aided 3D analytic tool was developed to characterize tumors after RF ablation. It involved a semiautomated 3D segmentation process that used a "tagged" watershed algorithm, which is described in Appendix E1 (*http://radiology.rsnajnls.org/cgi/content/full/2411050987/DC1*). This algorithm extended the "conventional" watershed algorithm available in the National Library of Medicine's Insight Segmentation and Registration Toolkit (*http://www.itk.org*). One abdominal radiologist (I.B., with 2 years of experience in abdominal radiology) segmented all ablated tumors for all 56 follow-up CT scans (for a total of 72 segmentations). The semiautomated tagged watershed algorithm allowed the 3D segmentations to be performed in, on average, 4 minutes with a standard laptop personal computer. Although the segmentations were semiautomated procedures, 42 (58%) of the 72 segmentations required only minimal user interaction. That is, only two mouse clicks were required—one in the ablated tumor and one in the surrounding liver parenchyma. These segmentations required 1 minute to perform.

After the ablated tumor was segmented, the resulting 3D object O was characterized quantitatively by its weighted volume, or WV(O). We considered G the center of gravity of object O, and vol the volume of a voxel in the image data. Then, the weighted volume WV(O) was defined by the following

Published online before print
10.1148/radiol.2411050987

Radiology 2006; 241:243–250

Abbreviations:
FDG = fluorine 18 fluorodeoxyglucose
RF = radiofrequency
3D = three-dimensional

Author contributions:
Guarantor of integrity of entire study, I.B.; study concepts/study design or data acquisition or data analysis/interpretation, all authors; manuscript drafting or manuscript revision for important intellectual content, all authors; approval of final version of submitted manuscript, all authors; literature research, I.B., R.K., P.R.M., E.V.; clinical studies, P.R.M., E.V., K.T., S.G.S.; experimental studies, R.K., E.V.; statistical analysis, I.B.; and manuscript editing, all authors

Authors stated no financial relationship to disclose.

summation among all voxels V contained in the ablated tumor O:

$$\mathrm{WV}(O) = \mathrm{vol} \cdot \sum_{V \in O} \|GV\|^2, \qquad (1)$$

where $\|GV\|$ is the distance between a voxel V and the center of gravity G of object O. This weighted volume was designed so that it would be more sensitive than a standard volume to changes that occurred in the periphery of the tumor.

During the period between two follow-up CT scans (CT_1 and CT_2) acquired at months m_1 and m_2, and given the assumption that the weighted volume of a particular ablated tumor varied from WV_1 to WV_2, we calculated the monthly growth of the weighted volume ($GR_{1\to2}$) as the following percentage (9):

$$GR_{1\to2} = [(WV_2/WV_1)^{1/(m_2-m_1)} - 1] \cdot 100. \qquad (2)$$

This percentage quantified the growth of the weighted volume in CT_2 by reference to its value in CT_1. So that it would be maximally sensitive for the detection of any new trend that occurred during the period ending at month m_2, CT_1 was chosen as the most recent prior CT scan available. Because only the ratio WV_2/WV_1 is involved, Equation (2) depends on relative rather than absolute values of WV_1 and WV_2.

Reference Standard Recurrence Assessment

In accordance with current practice (2,7) and because surgical resection of every ablated tumor would not be clinically acceptable, we used results of follow-up imaging, including PET, to determine whether an ablation was complete (range of total follow-up duration, 8–24 months [mean, 12.75 months]). PET scans were not performed at every follow-up time point; they were conducted only when requested by referring physicians. We reviewed all CT scans together with all PET scans obtained as follow-up to the RF ablation, and we derived retrospectively by consensus a reference standard for tumor recurrence (I.B.; S.G.S., with 16 years of experience in abdominal radiology). Recurrent tumor was defined as the presence of new abnormal enhancement at CT or new positive findings at PET. Whole-body dedicated PET (ECAT Exact HR+; CTI/Siemens, Knoxville, Tenn) was used to identify abnormal foci of hypermetabolism related to recurrent tumor. Scanning began 45–60 minutes after intravenous injection of 15–20 mCi (555–740 MBq) FDG. Recurrent tumor was identified in seven of 12 metastases; five tumors were considered to be completely ablated (Table).

Comparison of Detection with 3D Analytic Tool and Clinical Radiology Reports

One author (I.B.) tabulated radiology reports of CT findings by using a radiology information system (Impax; Agfa-Gevaert, Mortsel, Belgium). Interpretations, which were based solely on findings on transverse two-dimensional images, were rendered by one of four staff abdominal radiologists (including S.G.S. and K.T.) with 5–25 years of ex-

Characteristics of 12 Ablated Liver Tumors

Tumor No.	Tumor Size before Ablation (cm)	Patient Age (y)	Patient Sex	Primary Tumor	No. of Months after Ablation Follow-up CT Was Performed*	No. of Months after Ablation PET Was Performed†
1	2.9	63	F	Pancreatic neuroendocrine tumor	0, 3, 7, 10	10 (−)
2	3.4					
3	5.9	60	M	Gastrointestinal stromal tumor	0, 2, 5, 8, 12, 15	5, 15 (−)
4	2.6	52	M	Gastrointestinal stromal tumor	0, 1, 3, 4, 7, 8, 10, 13	1, 13 (−)
5	4.4	47	F	Gastrointestinal stromal tumor	1, 5, 6, 9,‡ 12‡	1, 6 (−), 9 (+)‡
6	5.1	63	M	Colon adenocarcinoma	0, 2,‡ 4,‡ 6,‡ 8,‡ 10‡	2 (+)‡
7	4.3					
8	2.9	73	M	Colon adenocarcinoma	0, 1,‡ 3,‡ 5,‡ 8‡	3 (+)‡
9	4.8	65	M	Gastrointestinal stromal tumor	0, 2,‡ 4,‡ 6,‡ 8,‡ 9,‡ 12,‡ 13,‡ 14‡	6 (+)‡
10	6.9	53	F	Malignant angiomyolipoma	0, 1,‡ 5,‡ 8‡	NA
11§	2.8	75	M	Colon adenocarcinoma	0, 3, 5, 12, 14, 18,‡ 19‡	18 (+)‡
12	2.3				0, 3, 5, 12, 14, 18, 21, 24	18, 24 (−)

* A CT examination at month 0 was a baseline postablation examination performed immediately after RF ablation.

† The presence or absence of tumor fluorine 18 fluorodeoxyglucose (FDG) uptake at PET is indicated by (+) or (−), respectively. NA = not applicable.

‡ Months when locally recurrent tumors were present, according to reference-standard recurrence assessment.

§ Tumor 12 did not recur and was followed up until month 24, whereas tumor 11 recurred and was re-treated with RF ablation at month 19 and thus excluded from longer follow-up.

perience. The date when a local recurrence was reported was noted. Cases with a discrepancy between clinical reports and 3D analytic tool results were identified. When both CT and PET were performed, we used initial CT reports by radiologists who were unaware of the PET results and who interpreted CT findings alone. In our practice, PET findings are compared with CT findings, and detailed information is given in the PET reports.

During a follow-up interval between months m_1 and m_2, the 3D analytic tool was considered to yield results negative for recurrence if the monthly growth value $GR_{1\rightarrow 2}$ (calculated with Eq [2]) was negative. The 3D analytic tool was considered to yield results positive for recurrence if the monthly growth value was positive. This 0% threshold represented an intuitive cutoff between a growing recurrent tumor (positive growth value) and an involuting completely ablated one (negative growth value). When the monthly growth value was positive but less than 5%, cases were considered as indeterminate, to take into account potential errors in our measurements.

For a global analysis of the evolution of each tumor, the results of all successive recurrence assessments associated with all follow-up intervals were considered. The follow-up interval (if any) when the monthly growth value became greater than 0% was identified as the time of recurrence, according to the 3D analytic tool.

Statistical Analysis

Because patients had variable durations of follow-up and either one or two tumors, we identified a homogeneous subset of 18 monthly growth values by using the following criteria: *(a)* For the three patients with two tumors, only one of the two tumors was considered. The selection of this specific tumor was randomly made, and we checked that all possible selections yielded the same statistical results. *(b)* For each patient, two monthly growth values, $V1$ and $V2$, were included to represent the monthly growth values computed during a period containing the postablation interval between months 3 and 4 and months 7 and 8, respectively. Months 3–4 and 7–8 were the intervals when data were available for every patient.

Statistical significance of the difference in monthly growth values between recurrent and nonrecurrent tumors at times $V1$ and $V2$ was then evaluated by using the analysis of variance F test (for analysis of variance between groups). The independence of this difference with respect to time $V1$ or $V2$ was verified. Differences were considered statistically significant if $P < .05$. Statistical software (Stata, release 9; Stata, College Station, Tex) was used.

Figure 1

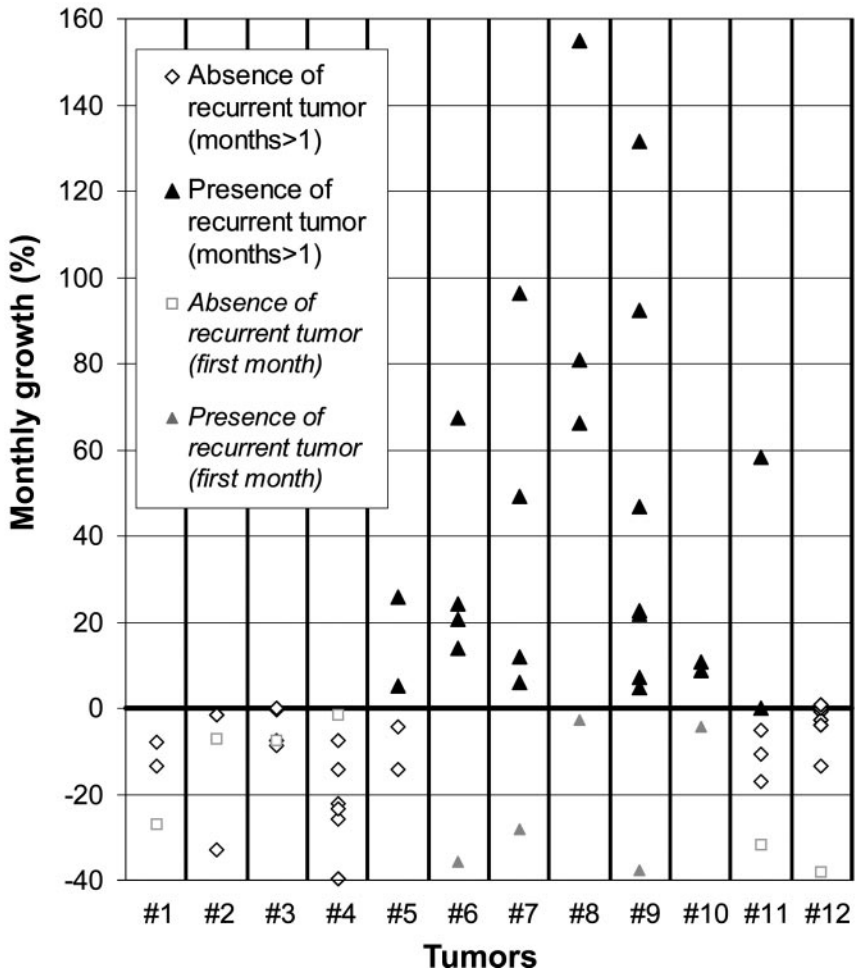

Figure 1: Graph shows weighted volume monthly growth values for all recurrent and completely ablated tumors. Each column shows all monthly growth values during all follow-up intervals for each tumor. When follow-up interval includes 1st month after RF ablation, all monthly growth values are negative (□, gray triangle). Beyond 1st month after RF ablation, absence of recurrent tumor (◇) is associated with monthly growth values lower than 0% (negative), while presence of recurrent tumor (▲) is associated with monthly growth values of 0% or greater (positive). Monthly growth values in presence of recurrent tumor were significantly different from monthly growth values in absence of recurrent tumor ($P < .01$).

Results

During every interval that included the 1st month after RF ablation, the 3D analytic tool showed negative monthly growth values for all metastases. No association was found between monthly growth values and the presence of recurrence. However, beyond the 1st month

after RF ablation, the absence of recurrent tumor was associated with negative monthly growth values, while the presence of recurrent tumor was associated with positive monthly growth values (Fig 1). This difference between recurrent and nonrecurrent tumor growth values was confirmed in the statistically tested homogeneous subset of data: Monthly growth values in the absence of recurrence were significantly different from monthly growth values in the presence of recurrence ($P = .015$). There was no dependence between this observation and the particular time point $V1$ or $V2$ when monthly growth was evaluated ($P < .140$).

Beyond the 1st month, when a threshold of 0% was used for the monthly growth value, the sensitivity for the detection of recurrent tumor for all 12 metastases with the 3D analytic tool was 100% (seven of seven), while the specificity was 60% (three of five). Two false-positive cases (tumors 3 and 12), both of which were in the indeterminate range of monthly growth values ($0\% \leq$ monthly growth $< 5\%$), were encountered. For all seven recurrent tumors, the follow-up interval when the monthly growth value became greater than 0% coincided with the time of the reference standard recurrence assessment.

The presence or absence of recurrent tumor was reported correctly by the radiologist with two-dimensional CT for 10 of 12 metastases. However, for the remaining two metastases, the 3D analytic tool detected a recurrence before it was reported clinically. In tumor 5, a change from a negative monthly growth value between months 5 and 6 (−4.4%) to a positive monthly growth value between months 6 and 9 (+5.1%) was associated with a late recurrence at month 9, as demonstrated with positive PET results (Fig 2). At that time, the recurrence had not been reported by the radiologist, and it was not detected until month 12. In tumor 11, the monthly growth value was indeterminate between months 14 and 18 (+0.15%). Recurrence was detected with PET at month 18 (Fig 3). This recurrence was not visible at CT and therefore was not detected until PET was performed.

Figure 2

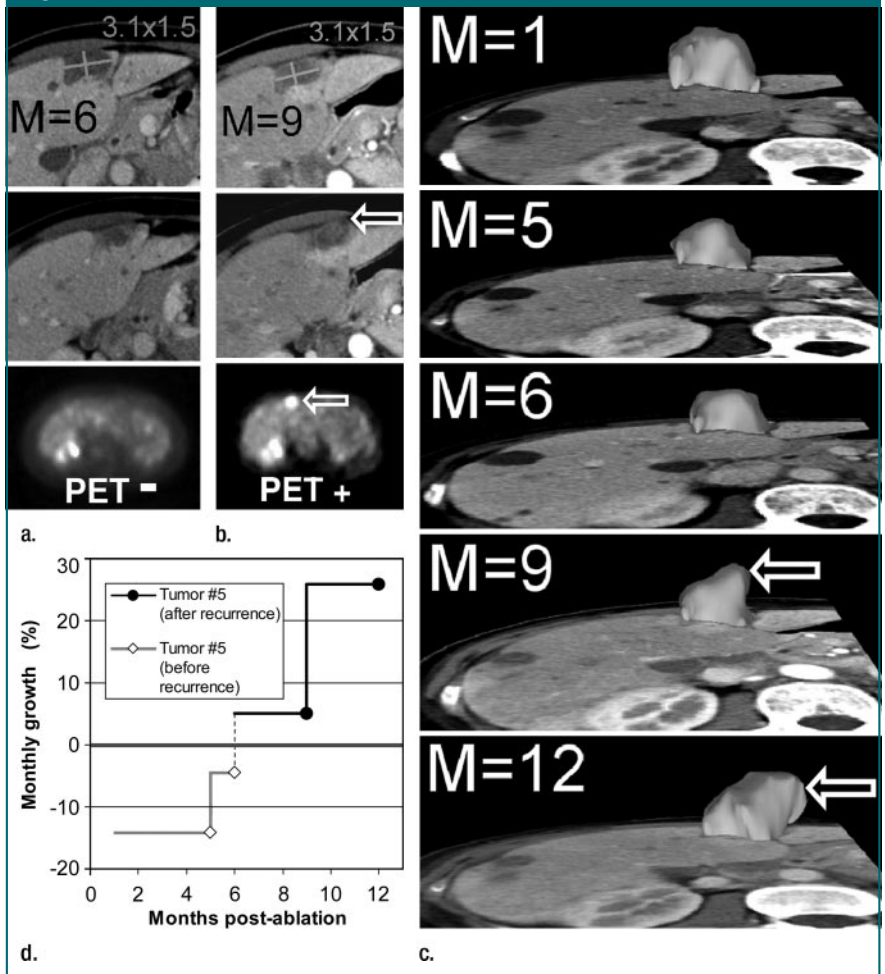

Figure 2: Monthly growth values and late recurrence 9 months after RF ablation in 47-year-old woman with 4.4-cm gastrointestinal stromal tumor metastasis (tumor 5). **(a)** Transverse CT (top and middle) and PET (bottom) images show that ablated tumor was 3.1 × 1.5 cm at month *(M)* 6 and did not have uptake at PET. **(b)** Transverse CT (top and middle) and PET (bottom) images show that maximal transverse dimensions were unchanged at month 9, with no abnormal enhancement. However, there was uptake at PET (arrow). Subtle change in tumor shape (arrow in middle) is related to recurrence. **(c)** Follow-up CT scans obtained 1, 5, 6, 9, and 12 months after RF ablation. Three-dimensional views of tumor on reference transverse plane show results of ablated tumor segmentations. Three-dimensional shape changes related to recurrence are seen at months 9 and 12 (arrows). **(d)** Graph shows evolution of monthly growth values. Weighted volume monthly growth values were computed during each of the follow-up intervals (1–5, 5–6, 6–9, and 9–12 months). Graph shows two monthly growth values before recurrence (◇) and two values after recurrence (●). Horizontal lines ending with ◇ or ● are interval during which each monthly growth value was computed. Change from negative to positive growth values at month 9 was associated with recurrence and change in status at PET.

Discussion

We developed and preliminarily evaluated a 3D analytic tool that can be applied to CT scans and used to evaluate treated tumor shapes. During every interval that included the 1st month after RF ablation, monthly growth values derived with the 3D tool were negative, regardless of the presence or absence of recurrent tumor. This initial decrease in

ablated tumor size was likely due to several factors including shrinkage of tumor, resolution of ablation-induced inflammation, and the fact that if residual tumor was present, it was likely too small to detect. Hence, the 3D tool had no value for assessing recurrence during the 1st month. Indeed, PET and CT are also limited soon after RF ablation because both FDG uptake and enhancement may be due to inflammation (5–8).

Evaluation of two-dimensional transverse CT scans, including the comparison of maximal transverse diameters, has limitations. Peripheral nodular recurrences may be subtle and therefore missed. Detection of changes in shape requires a precise section-by-section comparison with previous CT data. This can be difficult if section positions and orientations do not match between successive follow-up CT examinations. The use of multiplanar reformations may help, but analyzing many images can be time consuming for the radiologist.

After the 1st month following RF ablation, the 3D analytic tool proved helpful in quantifying ablated tumor shape variations and allowed recurrences to be detected even in the absence of abnormal enhancement. Monthly growth values computed by using the 3D analysis were significantly different in the absence of recurrent tumor from those in the presence of recurrent tumor.

The 3D analytic tool had a high sensitivity but a low specificity. Two false-positive cases were encountered in this study. Two completely ablated tumors showed slightly positive growth values (+0.10% for tumor 3 at month 15; +0.16% and +0.62% for tumor 12 at months 18 and 24, respectively). These false-positive cases could not be distinguished from case 11, where a PET-proved recurrence was associated with no abnormal enhancement and subtle morphologic changes that were not visible at CT (growth value, +0.15% during recurrence at month 18). Such cases, in which monthly growth values were positive but remained smaller than 5%, were defined as indeterminate. When recurrence cannot be detected with standard two-dimensional interpretation, 3D analysis may be able to reveal these indeterminate cases and prompt a PET scan to assess recurrence.

Our results might have been different if some patients had not undergone one of their follow-up CT examinations. For example, for tumor 11, whereas the monthly growth value became positive between months 14 and 18, a negative monthly growth value would have been computed between month 12 and 18 if data from the CT examination at month 14 had not been available. In this case, the recurrence would have been detected only at month 19. This illustrates the fact that recurrence detection may be delayed if intervals between two successive follow-up CT scans are lengthened.

The numeric values 0% and 5% were used to define the absence of recurrence (monthly growth value, <0%) and indeterminate cases (0% ≤ monthly growth value < 5%). Because we intended the 3D analytic tool to be used as an initial test for recurrence, we sought to maximize sensitivity by including all cases with positive growth values as positive. However, given potential errors in our measurements that were

Figure 3

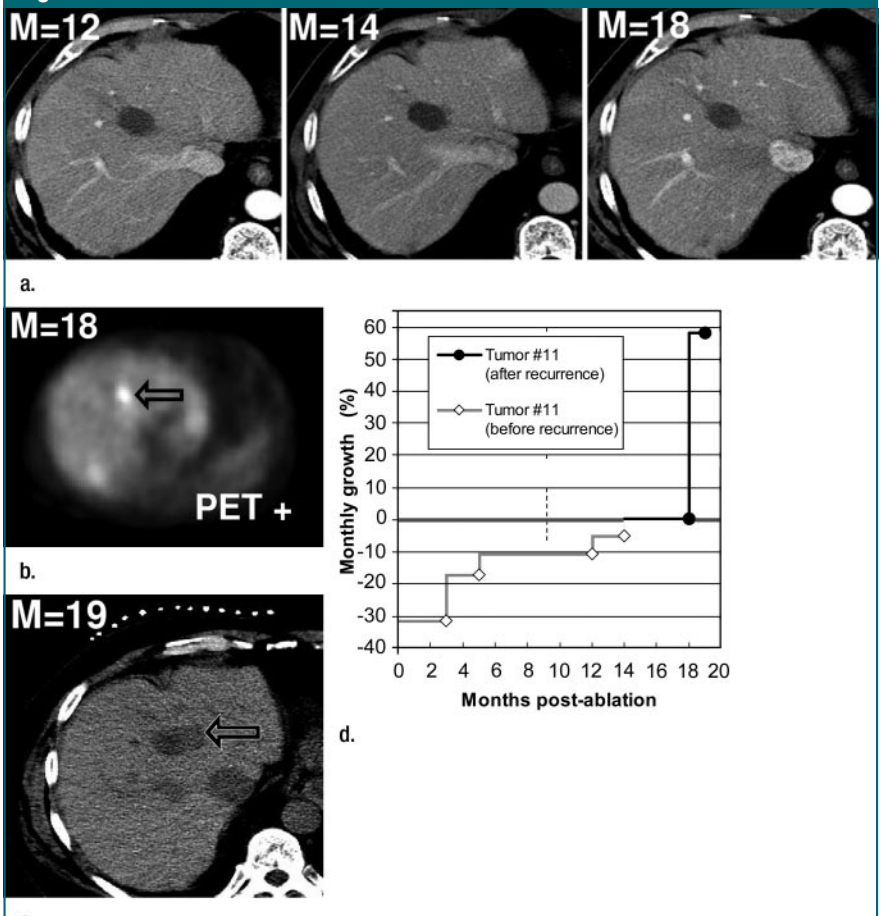

Figure 3: Monthly growth values and late recurrence 18 months after RF ablation in 75-year-old man with 2.8-cm colon adenocarcinoma metastasis (tumor 11). **(a)** On transverse follow-up CT scans at months *(M)* 12, 14, and 18, there were no detectable changes in ablated tumor morphology or enhancement, whereas **(b)** transverse PET scan at month 18 shows recurrence (arrow). Morphologic change on **(c)** nonenhanced CT scan, together with CT-guided biopsy results, confirmed recurrence (arrow) at month 19. **(d)** Graph shows that monthly growth value became slightly positive (+0.15%) between month 14 and 18—the month when PET revealed recurrence.

possibly responsible for false-positive cases, we considered positive cases with values less than 5% as indeterminate. Once these indeterminate cases are identified by the 3D tool, an additional test would be warranted before an invasive procedure such as biopsy or a new RF ablation is performed. The 0% and 5% thresholds proved to be effective in this study of 56 follow-up CT scans; in particular, 100% sensitivity and specificity of growth values less than 0% and 5% or greater were demonstrated. Nevertheless, the relatively small number of cases was a limitation of our study, and further work will be needed to validate our findings.

One abdominal radiologist supervised all segmentations of ablated tumors. We chose one observer because this technique is new; however, observer bias may have affected our results. We plan to analyze this tool by using multiple observers and assessing interobserver variability. To minimize single-observer bias, we chose to perform semiautomated segmentation of ablated tumors rather than manually segmenting them. Previous study results (10) have demonstrated that even a limited degree of automation has beneficial results with respect to intra- and interobserver variability. Although various segmentation algorithms could be used, results of previous comparative studies (10–12) have highlighted the watershed approach because it proved to be fast, stable, and able to generate accurate models. Watershed segmentation provides a flexible framework that allows users to interact with the segmentation process through a graphical interface. We believe that compared with the conventional watershed algorithm, our semiautomated tagged watershed algorithm is easier to use. This algorithm is an extension of the conventional watershed algorithm available in ITK, the National Library of Medicine's Insight Segmentation and Registration Toolkit (*http://www.itk.org*).

Lazebnik et al (13,14) presented a different approach to the quantitative characterization of RF-ablated tumors. Their aim was to compare MR imaging findings with histologic findings in the immediate postablation period. An ellipsoid model was fitted on ablated tumor boundaries. Our method, however, detects all shape changes, and was not restricted to an ellipsoid geometric model.

Various quantitative metrics may be calculated to characterize a 3D segmented ablated tumor (15). One of the simplest metrics would be the total volume of the tumor. We chose here to consider a weighted volume instead. We defined the weighted volume as a summation similar to a standard volume computation, but we added a weight function corresponding to the distance between each point of the ablated tumor and its center of gravity (Eq [1]). As a result, relative to standard volume, weighted volume was more sensitive to changes that occurred in the periphery of the tumor. This is particularly helpful because recurrences are more likely at the periphery of tumors (5–8). Therefore, we believe the "periphery sensitive" weighted volume is more appropriate than the standard volume in the detection of recurrence (16).

More complex approaches could be used to characterize the 3D shape of a tumor quantitatively. For example, spherical harmonics could provide a parametric 3D model of the segmented ablated tumor, and the temporal evolution of various indexes of shape could be computed from the spherical harmonics polynomial coefficients (17). However, we believe that the use of a greater number of clinically nonintuitive indexes to characterize a tumor's shape is less robust than the use of the single weighted volume criterion. Nevertheless, these alternative approaches warrant more research.

Limitations of our study included the small number of patients and lesions, which limited the value of statistical analysis; the heterogeneity of the tumor origins; and the fact that the reference standard for tumor recurrence was PET and follow-up imaging rather than surgical resection of every ablated tumor.

In conclusion, after the 1st month following percutaneous RF ablation, a computer-aided 3D analytic tool may prove useful in analyzing the shape of ablated liver tumors and identifying recurrences. We believe that the following strategy can be considered when CT scans show no abnormal enhancement beyond the 1st month after RF ablation: The weighted volume monthly growth value could be computed by using a previous follow-up CT scan. CT scanning coupled with the 3D tool assessment could be used as an initial test for local recurrence, and, when both yield negative results, further investigations such as PET or biopsy would be unnecessary: A negative monthly growth value would increase the confidence that there is no recurrence. However, when the 3D tool reveals a positive monthly growth value greater than 5%, a percutaneous biopsy would be warranted, as well as an additional RF ablation session, if indicated. Cases in which monthly growth values are positive but smaller than 5% might warrant a PET scan. We realize that our results are preliminary; additional evaluation will be needed before this 3D analytic tool is used in clinical practice.

Acknowledgments: We acknowledge Jean-Luc Bosson, MD, PhD, and the Clinical Research Center INSERM 003 of Grenoble University Hospital for contributions to statistical analysis of data.

References

1. Vogl TJ, Muller PK, Mack MG, Straub R, Engelmann K, Neuhaus P. Liver metastases: interventional therapeutic techniques and results, state of the art. Eur Radiol 1999;9:675–684.
2. Solbiati L, Livraghi T, Goldberg SN, et al. Percutaneous radio-frequency ablation of hepatic metastases from colorectal cancer: long-term results in 117 patients. Radiology 2001;221:159–166.
3. de Baere T, Risse O, Kuoch V, et al. Adverse events during radiofrequency treatment of 582 hepatic tumors. AJR Am J Roentgenol 2003;181:695–700.
4. Gazelle GS, Goldberg SN, Solbiati L, Livraghi T. Tumor ablation with radio-frequency energy. Radiology 2000;217:633–646.
5. Dromain C, de Baere T, Elias D, et al. Hepatic tumors treated with percutaneous radio-frequency ablation: CT and MR imaging follow-up. Radiology 2002;223:255–262.
6. Kim SK, Lim HK, Kim YH, et al. Hepatocellular carcinoma treated with radio-frequency

ablation: spectrum of imaging findings. RadioGraphics 2003;23:107–121.

7. Choi H, Loyer EM, DuBrow RA, et al. Radiofrequency ablation of liver tumors: assessment of therapeutic response and complications. RadioGraphics 2001;21(Spec Issue): S41–S54.

8. Chopra S, Dodd GD 3rd, Chintapalli KN, Leyendecker JR, Karahan OI, Rhim H. Tumor recurrence after radiofrequency thermal ablation of hepatic tumors: spectrum of findings on dual-phase contrast-enhanced CT. AJR Am J Roentgenol 2001;177:381–387.

9. Barrie Wetherill G. Elementary statistical methods. London, England: Methuen, 1967.

10. Bellon E, Feron M, Maes F, et al. Evaluation of manual vs semi-automated delineation of liver lesions on CT images. Eur Radiol 1997; 7:432–438.

11. Rogowska J, Batchelder K, Gazelle GS, Halpern EF, Connor W, Wolf GL. Evaluation of selected two-dimensional segmentation techniques for computed tomography quantitation of lymph nodes. Invest Radiol 1996; 31:138–145.

12. Wust P, Gellermann J, Beier J, et al. Evaluation of segmentation algorithms for generation of patient models in radiofrequency hyperthermia. Phys Med Biol 1998;43:3295–3307.

13. Lazebnik RS, Weinberg BD, Breen MS, Lewin JS, Wilson DL. Three-dimensional model of lesion geometry for evaluation of MR-guided thermal ablation therapy. Acad Radiol 2002;9:1128–1138.

14. Lazebnik RS, Breen MS, Lewin JS, Wilson DL. Automatic model-based evaluation of magnetic resonance-guided radio frequency ablation lesions with histological correlation. J Magn Reson Imaging 2004;19:245–354.

15. Silverman SG, Sun MR, Tuncali K, et al. Three-dimensional assessment of MRI-guided percutaneous cryotherapy of liver metastases. AJR Am J Roentgenol 2004;183: 707–712.

16. Bricault I, Kikinis R, vanSonnenberg E, Tuncali K, Silverman SG. 3D analysis of radiofrequency-ablated tumors in liver: a computer-aided diagnosis tool for early detection of local recurrences. In: Barillot C, Haynor DR, Hellier P, eds. Medical image computing and computer-assisted intervention: 7th international conference—lecture notes in computer science. Vol 3217. Berlin, Germany: Springer-Verlag, 2004; 1042–1043.

17. Goldberg-Zimring D, Achiron A, Guttmann CR, Azhari H. Three-dimensional analysis of the geometry of individual multiple sclerosis lesions: detection of shape changes over time using spherical harmonics. J Magn Reson Imaging 2003;18:291–301.